World J Microbiol Biotechnol (2017) 33:163
DOI 10.1007/s11274-017-2329-z

ORIGINAL PAPER

Relationship between salt tolerance and nanoparticle synthesis by *Williopsis saturnus* NCIM 3298

Pallavi Mohite[1] · Ameeta Ravi Kumar[1] · Smita Zinjarde[1,2]

Received: 6 April 2017 / Accepted: 1 August 2017 / Published online: 5 August 2017

Abstract This work describes cell associated and extracellular synthesis of nanoparticles by the yeast, *Williopsis saturnus*. The yeast was able to grow in the absence and presence of sodium chloride (NaCl) and form nanoparticles in a cell associated manner. The content of melanin, a stress-associated pigment was found to be progressively greater in the presence of increasing concentrations of NaCl. With higher quantities of melanin (extracted from yeast cells grown in the presence of 4% of NaCl), smaller sized nanoparticles were obtained. This is the first report on understanding the relationship between halotolerance, production of a stress-related pigment (melanin) and synthesis of nanoparticles with antioxidant properties by using *W. saturnus* as a model system. The cell free extracts derived from cultures grown in the absence of NaCl were able to mediate extracellular synthesis of gold and silver nanoparticles and the biomolecule mediating nanoparticle synthesis was identified to be a glycolipid. Extracellularly synthesized gold nanoparticles displayed good catalytic activity and rapidly mediated the reduction of 4-nitrophenol to 4-aminophenol.

Keywords Glycolipid · Halotolerance · Melanin · Nanoparticles · *Williopsis saturnus*

Electronic supplementary material The online version of this article (doi:10.1007/s11274-017-2329-z) contains supplementary material, which is available to authorized users.

✉ Smita Zinjarde
smita@unipune.ac.in

[1] Institute of Bioinformatics and Biotechnology, Savitribai Phule Pune University, Pune, Maharashtra 411007, India

[2] Department of Microbiology, Savitribai Phule Pune University, Pune, Maharashtra 411007, India

Introduction

Nanotechnology deals with matter at the nanometer scale. This science is interdisciplinary and involves inputs from the fields of physics, chemistry, biology, and material science. Nanoparticles (NPs) exhibit unusual optical, chemical, photo-electrochemical and electronic properties. They are used as antibacterial agents, in drug delivery, cancer therapy, catalysis, manufacture of cosmetics and in the development of sensors (Moghaddam et al. 2015; Balakumaran et al. 2016). Several synthetic protocols have been designed to obtain different type of nanoparticles. Bacteria, filamentous fungi, yeasts, algae and plants from different environments have been exploited for this purpose (Singh et al. 2016).

Yeasts are advantageous for developing nanosynthetic bioprocess as they secrete large quantities of extracellular proteins and other biomolecules. Literature survey reveals that yeast genera such as *Candida, Cryptococcus, Magnusiomyces, Pichia, Rhodosporidium, Rhodotorula, Saccharomyces, Schizosaccharomyces, Schwanniomyces, Torulopsis* and *Yarrowia* mediate the synthesis of metal nanoparticles (Kowshik et al. 2002a, b; Jha et al. 2009; Mohite et al. 2015, 2016; Singh et al. 2016; Zhang et al. 2016). Among these genera, *Cryptococcus, Schwanniomyces, Yarrowia, Pichia* and *Schizosaccharomyces* are known to be halotolerant.

Microorganisms isolated from natural salt-containing environments maybe halophilic or halotolerant. Although halotolerant microorganisms do not require salt for carrying out life processes, they rapidly adapt to the presence of high salt contents in the environment (Oren 2002). In order to endure these extremities, halotolerant yeasts often produce compatible solutes such as polyols or pigments like melanin (Gunde-Cimerman et al. 2000). These molecules

have the ability to interact with metals and form nanoparticles (Nghia et al. 2012; Khodashenas and Ghorbani 2015). As stated earlier a few halotolerant yeast genera are capable of synthesizing nanoparticles. However, these reports do not detail the effect of salinity on the production of biomolecules that can mediate synthesis of nanoparticles. In the current study, the hitherto unreported halotolerant yeast *Williopsis saturnus* was used as a model system to understand this relationship. *W. saturnus* is a biotechnologically relevant halotolerant yeast species (Peng et al. 2009; Kamat et al. 2013). Literature survey shows that there are a few reports on metal interactions related to this yeast (Vadkertiova and Slavikova 2006; Bhattacharya et al. 2015). It was thus hypothesized that *W. saturnus* may be a potential candidate for studying the effect of salt on synthesis of NPs. It was hypothesized that for cell associated nanoparticle formation by this yeast, the presence of NaCl would enhance synthesis of melanin pigment and increased melanin content could result in the formation of nanoparticles with different morphological properties. This work details (i) the halotolerant nature of *W. saturnus* strain NCIM 3298, (ii) describes cell associated and extracellular nanoparticle synthesis by this yeast, (iii) understands the mechanism by which both these type of NPs are synthesized and (iv) discusses antioxidant and catalytic properties of the melanin- and glycolipid-stabilized nanoparticles, respectively.

Materials and methods

Organism and growth conditions

Williopsis saturnus var. *saturnus* NCIM 3298 was obtained from National Collection of Industrial Microorganisms (NCIM), National Chemical Laboratory, Pune, India. The culture was maintained on MGYP agar [malt extract, 3.0; glucose, 10.0; yeast extract, 3.0; peptone, 5.0; agar, 20.0 (g/L of distilled water)] and sub-cultured at monthly intervals.

Experimental conditions

Effect of NaCl on growth of *W. saturnus*

Cells were cultivated in MGYP or YNBG [yeast nitrogen base, 7.0; D-glucose, 10.0 (g/L of distilled water)] in the presence of sodium chloride (NaCl) at different concentrations (0–4.0%). The effect of NaCl on growth was monitored by checking Absorbance at 600 nm (A_{600}) after 72 h of incubation at 30 °C on a shaker.

Effect of NaCl on nanoparticle synthesis and electron microscopic observations

Yeast cells were grown in the presence or absence of NaCl in MGYP medium and incubated for 72 h at 30 °C under shaking conditions. The liquid cultures were centrifuged at 6000×*g* at 4 °C; pellets were washed thrice and resuspended to contain 10^{10} cells/mL. Synthesis of cell associated gold nanoparticles was monitored by incubating 0.5 mL of cell suspensions with equal volumes of 1 mM tetrachloroauric acid ($HAuCl_4$) at different temperatures (30, 40, 50, 60, 80 °C or boiling water bath). Cell associated nanoparticles were observed by using an analytical field emission scanning electron microscope (FESEM). The biosynthesized nanoparticles were mounted on silicon wafers (1 cm × 1 cm) and dried overnight. Platinum coated samples were analyzed by using a FESEM (FEI Nova Nano SEM 450) equipped with an energy dispersive spectrometer (EDS).

Characterization of nanoparticles

For transmission electron microscope (TEM) analysis, samples were immobilized on carbon-coated copper grids (200 µm mesh size) and the model used was a Tecnai G2 20U Twin (FEI, Netherlands) equipped with selective electron diffraction (SAED) attachment. For X-ray diffraction (XRD) measurements, films of nanoparticles were made by drop-coating on Si wafers. XRD patterns were recorded on a D8 Advanced Brucker instrument in the transmission mode with Cu Kα radiation and $\lambda = 1.54$ Å.

Extraction of cell associated melanin and melanin mediated synthesis of NPs

The presence of NaCl is known to have an impact on pigmentation in certain fungi (Tresner and Hayes 1971). For carrying out these experiments, *W. saturnus* was grown in the absence or presence of different concentrations of NaCl. Cell associated melanin was obtained by following a standard protocol (Ito et al. 2007). Commercially available melanin (Sigma Aldrich, India) was appropriately diluted and values of Absorbance at 430 nm (A_{430}) versus concentration were plotted. Melanin was quantified on the basis of this plot. Fourier transform infrared (FTIR) profiles of isolated and standard melanin were obtained on a Shimadzu FTIR spectrophotometer (FTIR 8400). Spectra were collected at resolution of 4 cm^{-1} in the transmission mode (4000–400 cm^{-1}). The solubility of the extracted pigment in 1 N NaOH, 1 N KOH or organic solvents and bleaching with NaOCl and H_2O_2 was also checked.

Nanoparticles were synthesized by incubating extracted melanin [derived from cells grown in the

presence of different concentrations of NaCl (0–4%)] with 1 mM $HAuCl_4$ or silver nitrate ($AgNO_3$) solutions in a boiling water bath for 10 min. Visual changes and UV–Visible spectra were recorded. The synthesized nanoparticles were characterized on the basis of TEM observations.

Formation of extracellular NPs and characterization of glycolipid involved in NP synthesis

For these experiments, the yeast was grown in YNBG liquid medium (to prevent interference from organic media ingredients) containing different concentrations of NaCl (0–4%) at 30 °C for 120 h on a shaker. A longer period of incubation was used to ensure complete utilization of glucose. Cell free supernatants (CFS) were obtained by centrifugation of the liquid culture at 6000×*g* and they were evaluated for synthesis of gold nanoparticles (AuNPs) and silver nanoparticles (AgNPs). Equal volumes (0.5 mL) of CFS were incubated with 1 mM $HAuCl_4$ or $AgNO_3$ in a boiling water bath for 15 min. In control experiments, the CFS was replaced with distilled water. Synthesis of nanoparticles was monitored visually (color change) and by UV–Visible spectroscopy by using a dual-beam spectrophotometer model Jasco V-530. Since nanoparticle synthesis was observed only in the absence of NaCl, for further studies the CFS derived from cells grown in the absence of salt were used. The effect of different parameters on NP synthesis was monitored by changing one variable at a time. Parameters studied were time (0, 5, 10, 15, 20, 25 and 30 min); temperature (30, 40, 60, 80 °C and boiling water); $HAuCl_4$ or $AgNO_3$ concentration (1.0, 2.0, 3.0 or 4.0 mM) and ratios of the $HAuCl_4$ or $AgNO_3$ to the CFS (1:1, 1:2, 1:3 or 1:4, 1:5). Optimum conditions were decided on the basis of the intensity of peaks around 540 and 410 nm for AuNPs and AgNPs, respectively. The biologically synthesized nanoparticles were characterized by TEM observations and XRD studies.

For identifying the biomolecule involved in NP synthesis, the protocol reported by Sowani et al. (2016a) was used. Briefly, *W. saturnus* was grown in a minimal medium (YNBG) to avoid interference from media components. The CFS was extracted with chloroform: methanol concentrated and loaded onto thin layer chromatography (TLC) plates (silica gel 60 F_{254}, Merck). Orcinol-sulphuric acid and ninhydrin staining, respectively were used to locate glycolipid and lipopeptide bands (Sprott et al. 2003). Portions of these plates were also sprayed with 1 mM chloroauric acid and development of purple color helped in the purification of the active component. The residual aqueous portion was also evaluated for NP synthesis. The purified glycolipid was acid hydrolyzed and the sugar and fatty acid components were identified on the basis of GC-MS analysis by following a protocol described earlier (Mohite et al. 2016).

Synthesis and characterization of nanoparticles mediated by purified glycolipid

Purified glycolipid samples were incubated with 1 mM $HAuCl_4$ or $AgNO_3$. Control tubes contained distilled water instead of the glycolipid. The reaction mixtures were incubated in a boiling water bath for 10 min. Characterization of nanoparticles was done by TEM and XRD. The effect of NaCl on nanoparticle synthesis by the purified glycolipid was also checked. Aliquots of purified glycolipid were incubated with $HAuCl_4$ in the absence and presence of NaCl (0, 1, 2, 3, 4 or 5%) and synthesis of AuNPs was monitored.

Applications of nanoparticles

Antioxidant activity of melanin-stabilized nanoparticles

The antioxidant activities of NPs derived from extracted melanin were studied by using the 1,1-Diphenyl-2-picrylhydrazyl (DPPH) assay. To 100 µL of samples (AuNPs and AgNPs synthesized by using melanin derived from *W. saturnus* grown in the presence of different concentrations of NaCl), 50 µL of DPPH solution (0.01 mM, prepared in methanol) was added. Absorbance at 517 nm (A_{517}) after 40 min was noted by using methanol as the blank reaction (Mittal et al. 2012). The DPPH free radical scavenging activity was calculated by using the following formula:

$$\text{Scavenging activity } (\%) = \frac{(\text{Ac} - \text{As}) \times 100}{\text{Ac}}$$

where Ac and A_S are values for A_{517} with DPPH and DPPH after reaction with sample, respectively.

Reduction of 4-nitrophenol by extracellular AuNPs and AgNPs

Extracellular nanoparticles obtained from *W. saturnus* were used as catalysts for bringing about reduction of 4-nitrophenol (4-NP) to 4-aminophenol (4-AP). Aqueous $NaBH_4$ solution (0.3 M, 1.5 mL) was added to 0.5 mL of 4-NP aqueous solution (0.03 mM). Aliquots of biosynthesized AuNPs or AgNPs (2 mL) were introduced into the reaction mixtures and time dependent absorption spectra were recorded at intervals of 2 min in the range of 200–600 nm. The progress of reaction was monitored by using a Perkin–Elmer Lambda-5 Spectrophotometer. The reactant, 4-NP and the product 4-AP displayed different absorption

spectra in the UV–Visible region and this feature was used to monitor the progress of the reaction. The kinetic rate constant of the reduction reaction was calculated by analyzing the change in an intensity of the peaks at 400 nm as a function of time.

All experiments were performed in triplicates with two biological replicates. Average values with standard deviation are depicted in graphs and representative images have been included.

Results

Effect of NaCl on the growth and nanoparticle synthetic ability of *W. saturnus*

As stated earlier, strains of *W. saturnus* are known to be halotolerant and are found in salt containing samples such as mangrove wetlands and salted foods. To study the effect of salt on growth, *W. saturnus* was cultivated in rich and minimal media (MGYP and YNBG, respectively) in the absence and presence of NaCl. Figure 1 shows the growth of *W. saturnus* in media containing different concentrations (0–4%) of NaCl. In MGYP, NaCl concentrations up to 4% supported growth. In YNBG, no growth was observed beyond 1% of NaCl. For further studies related to cell associated nanoparticle synthesis, MGYP medium was used.

Effect of NaCl on cell associated synthesis of nanoparticles was checked. For this, the yeast was grown in the absence or in the presence of 4% NaCl for 72 h. The yeast biomass obtained under both the conditions was harvested; cells were resuspended to contain 10^9 cells/mL and incubated with 1 mM $HAuCl_4$ for 15 min. The nanoparticle loaded cells were observed by using a FESEM. Figure 2a shows gold nanoparticles associated with cells grown in the absence of NaCl (white arrows). Cells grown in the presence of NaCl were smaller and also formed cell associated AuNPs (Fig. 2b, white arrows). Some dislodged nanoparticles were observed.

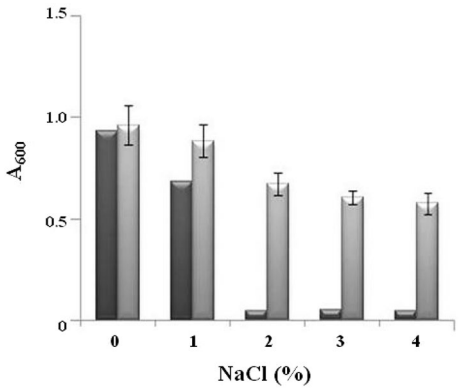

Fig. 1 Effect of NaCl on the growth of *W. saturnus* NCIM 3298 (YNBG: *dark gray*; MGYP: *light gray*)

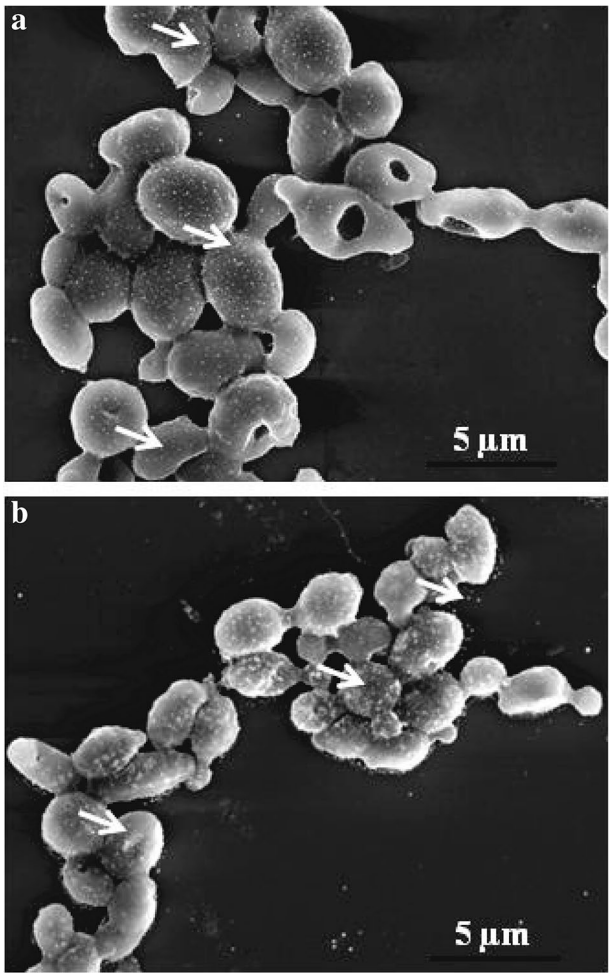

Fig. 2 FESEM images of *W. saturnus* NCIM 3298 incubated with $HAuCl_4$ showing the presence of AuNPs obtained from biomass grown in the **a** absence of NaCl **b** presence of 4% NaCl (*white arrows* point towards the nanoparticles)

Quantitation of melanin obtained from *W. saturnus* grown in the presence of NaCl

As hypothesized earlier, it was thought that *W. saturnus* grown in the presence of salt would produce enhanced quantities of pigments such as melanin. To test the hypothesis with *W. saturnus*, melanin associated with a fixed biomass weight (grown in the presence of increasing concentrations of NaCl) was extracted. The melanin content in the absence of NaCl was around 66 mg/g biomass. This was found to increase as concentration of NaCl was increased (Fig. S1, supplementary material). With the highest concentration of NaCl supporting growth (4%), the melanin content was found to be around 165.2 mg/g biomass.

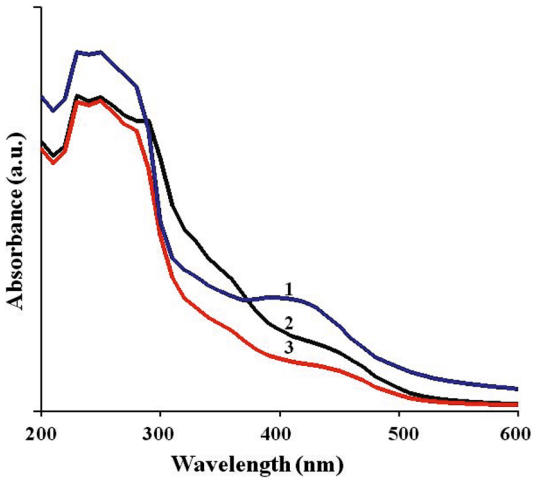

Fig. 3 UV–Visible spectra of melanin samples. (*1*) standard melanin; (*2*) with 0%; (*3*) with 4% NaCl

Table 1 Frequency analysis and group assignment of FTIR bands for extracted and synthetic melanin

Wavenumber (cm^{-1})	Functional groups
3400	O–H
1634	N–H
1110	C–N
2917, 2839 and 1300	Aliphatic C–H
700	Out-of-plane bending of the aromatic carbon-hydrogen bonds in melanin

All the pigment samples were normalized with respect to melanin content and UV–Visible spectra were obtained. A scan of standard melanin is depicted in Fig. 3 (line1). Representative scans of melanin samples obtained from cells grown in the absence and presence of 4% NaCl are also shown in Fig. 3 (lines 2 and 3, respectively). The test and standard samples displayed spectra with characteristic peaks in the range between 230 and 300 nm. As anticipated, the extraction protocol resulted in the isolation of melanin. FTIR profiles of samples obtained from cells grown in the absence and presence of 4% NaCl and standard melanin were obtained and the frequency analysis and group assignment of FTIR bands for extracted and synthetic melanin are shown in Table 1. Bands typical for melanin were obtained. The pigment was soluble in 1 N NaOH or KOH but was insoluble in water and organic solvents (ethanol, chloroform or acetone). It was bleached after treatment with NaOCl and H_2O_2.

Synthesis and characterization of melanin-stabilized AuNPs and AgNPs

All samples of melanin (extracted from cells grown in the presence of different concentrations of NaCl) formed nanoparticles. UV–Vis spectra of AuNPs and AgNPs are shown in Fig. S2 (supplementary material). Peaks characteristic of AuNPs and AgNPs (at 520 and 420 nm, respectively) were observed (lines 1–5). Such specific peaks were not observed with control samples (line 6).

TEM images of AuNPs and AgNPs synthesized by using melanin (extracted from cells grown in the absence and presence of NaCl at a concentration of 4%) are shown in Fig. 4. In this set of experiments, the melanin obtained as such was used without normalizing concentrations. It must be noted that in the absence of NaCl, melanin content was lower and with 4% NaCl, it was higher (Fig. S1, supplementary material). From Fig. 4a, it is evident that the size of AuNPs synthesized by using melanin extracted from cells grown without NaCl were spherical and around 20–30 nm in size. With melanin samples extracted from cells grown in the presence of 4% NaCl, AuNPs were smaller in the range between 5 and 15 nm (Fig. 4b). TEM images of silver nanoparticles synthesized by using extracted melanin (with and without NaCl) are shown in Fig. 4c, d, respectively. Melanin obtained from cells grown in the absence of NaCl mediated the synthesis of AgNPs that were spherical and in the range of 10–20 nm (Fig. 4c). When melanin samples derived from cells grown in the presence of NaCl were used, monodisperse NPs with a smaller size (5–15 nm) were observed (Fig. 4d). Selective electron diffraction (SAED) pattern of polycrystalline AuNPs and AgNPs synthesized by melanin extracted from cells grown in the absence and presence of NaCl, respectively, are shown in Fig. 4 as insets.

Synthesis and characterization of extracellular AuNPs and AgNPs obtained from CFS

CFS obtained from cells grown in YNBG medium containing NaCl did not form NPs. However, CFS derived from media lacking NaCl formed nanoparticles when incubated with $HAuCl_4$ or $AgNO_3$ (Fig. S3, supplementary material). Control reactions did not show colors or peaks characteristic of nanoparticles (Fig. S3a, b; lines and tubes 1). Test reactions developed distinct purple and brown colors and UV–Visible spectra displayed characteristic peaks at 540 and 420 nm typically indicating the synthesis of AuNPs and AgNPs, respectively (Fig. S3a and b, lines and tubes 2). Optimum conditions for NP synthesis were as follows: time: 15 min; temperature: incubation in a boiling water bath; concentration of $HAuCl_4$ or $AgNO_3$: 1 mM; ratio of CFS to $HAuCl_4$ or $AgNO_3$: 1:1. As stated earlier, the CFS

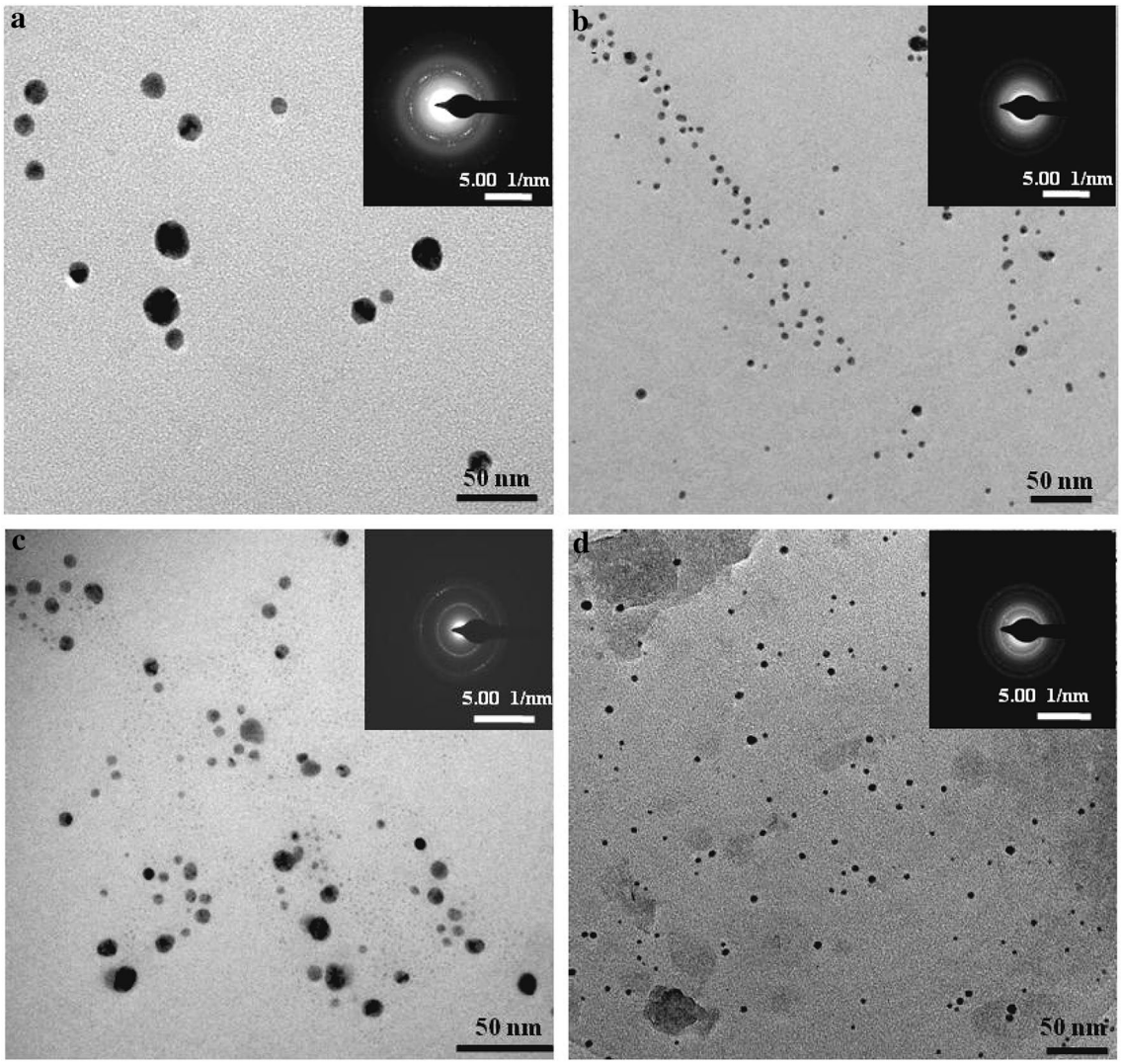

Fig. 4 Characterization of AuNPs and AgNPs synthesized by melanin extracted from cells of *W. saturnus*. Representative TEM images of **a** AuNPs (without NaCl), **b** AuNPs (with 4% NaCl), **c** AgNPs (without NaCl), **d** AgNPs (with 4% NaCl). *Insets* SAED patterns of respective NPs

obtained from cells grown in the presence of NaCl did not form NPs indicating the role of a salt sensitive biomolecule in synthesis of NPs.

Figure 5 depicts the characteristics of AuNPs and AgNPs synthesized by the CFS of *W. saturnus* under optimum conditions. XRD analysis was carried out to study the crystal structure of the biosynthesized metal nanoparticles. Figure 5a is a representative XRD pattern of AuNPs synthesized under optimized conditions. The peaks due to (1 1 2), (1 1 1), (2 0 0) and (2 2 0) Bragg reflections at 2θ values of 31.7, 38.2, 44.5 and 64.7°, respectively were observed (JCPDS No. 04-0784). The face-centered cubic (fcc) crystalline nature of the NPs was confirmed from this analysis. A representative TEM image of AuNPs synthesized by CFS of *W. saturnus* under optimum conditions is depicted as an inset in Fig. 5a. The AuNPs were spherical or hexagonal and ranged in size from 20 to 35 nm. XRD patterns of AgNPs showed four intense peaks in the spectrum at 38.1, 45.3, 64.2 and 77.4° (Fig. 5b). These could be indexed to crystalline planes of fcc silver (1 1 1), (2 0 0), (2 2 0) and (3 1 1), respectively (JCPDS 04-0783). These values are in agreement with XRD profiles observed with other biogenic silver nanoparticles. A representative TEM image (Fig. 5b, inset) shows the presence of well dispersed predominantly spherical nanoparticles in the range of 5 to 20 nm.

Isolation and identification of biomolecule mediating extracellular NP synthesis

As NP synthesis was observed within a short period of incubation at higher temperatures, it was understood that

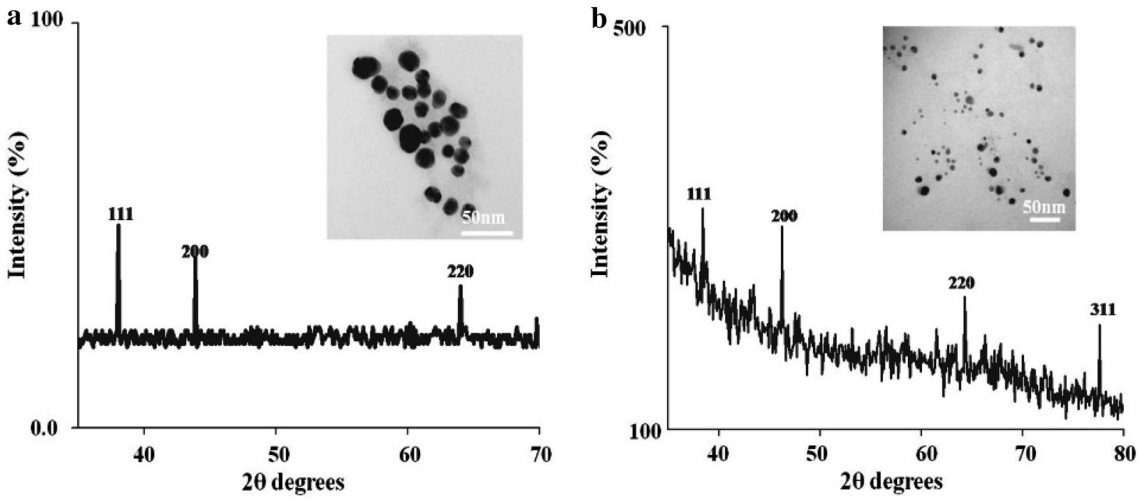

Fig. 5 Characterization of extracellular AuNPs and AgNPs synthesized by CFS of *W. saturnus* **a** XRD profile of AuNPs (*inset*: TEM image), **b** XRD profile of AgNPs (*Inset*: TEM image)

some heat resistant moiety was carrying out the reduction reactions. When the organic phase was concentrated, subjected to preparative TLC, staining with orcinol reagent, a band with an R_f value of 0.55 indicating the presence of a glycolipid was observed. With ninhydrin, no band was observed. Another part of the TLC plate was treated with $HAuCl_4$ and a band with same R_f value (0.55) turned purple suggesting that the glycolipid was bringing about reduction of chloroauric acid. NPs were not formed by the residual aqueous phase. The glycolipid mediating nanoparticle synthesis was characterized. Based on retention times of TMS derivatives of components present in the aqueous phase, mass fragmentation patterns and comparison with the NIST library, the sugar was identified as glucose. The hexane fraction after methyl esterification showed the presence of palmitic and stearic acid as the major fatty acid components. On the basis of the peak areas, the proportion of palmitic acid: stearic acid was found to be 3:1.

Synthesis and characterization of glycolipid-stabilized AuNPs and AgNPs

Initial studies indicated that the glycolipid obtained from *W. saturnus* mediated the synthesis of AuNPs (seen as a purple colored band on TLC plates when challenged with aqueous $HAuCl_4$). To confirm these findings, purified glycolipid samples were incubated in a boiling water bath with 1 mM $HAuCl_4$ or $AgNO_3$ solutions. UV–Visible spectra of AuNPs and AgNPs showed characteristic peaks at 540 and 410 nm, respectively (Fig. S4, supplementary information). Tubes containing AuNPs or AgNPs are shown as insets.

Representative TEM images of AuNPs and AgNPs formed by the purified glycolipid are depicted in Fig. 6a, c, respectively. From the TEM image in Fig. 6a, it is clear that AuNPs formed by using the purified glycolipid were mainly spherical with a size that ranged between 10 and 20 nm. AgNPs were found to be smaller. With the purified glycolipid, only spherical nanoparticles were observed. XRD patterns of the nanoparticles confirmed their polycrystalline nature. Glycolipid-mediated AuNPs exhibited three peaks with 2θ values of 38.5, 44.65 and 65° that correspond to the (1 1 1), (2 0 0) and (2 2 0) planes, respectively, of face centered cubic (fcc) gold crystals (Fig. 6b). As seen in Fig. 6d, silver nanoparticles showed peaks at 2θ values of 38.1, 46.48 and 64.60° corresponding to the (1 1 1), (2 0 0) and (2 2 0) planes of fcc silver crystals, respectively.

The glycolipid derived from *W. saturnus* thus mediated the synthesis of nanoparticles without the addition of any other reducing or capping agents. The nanoparticle synthetic abilities of purified glycolipid were also studied in the presence of NaCl. On the basis of UV–Visible spectra and visual observations it was evident that glycolipid stabilized AuNPs were synthesized only in the absence of NaCl (Fig. S5).

Application of melanin and glycolipid stabilized NPs

DPPH radical scavenging activity of NPs synthesized from extracted melanin

The results of DPPH free radical scavenging activity by nanoparticles are shown in Fig. S6 (supplementary material). All samples showed antioxidant activity. DPPH

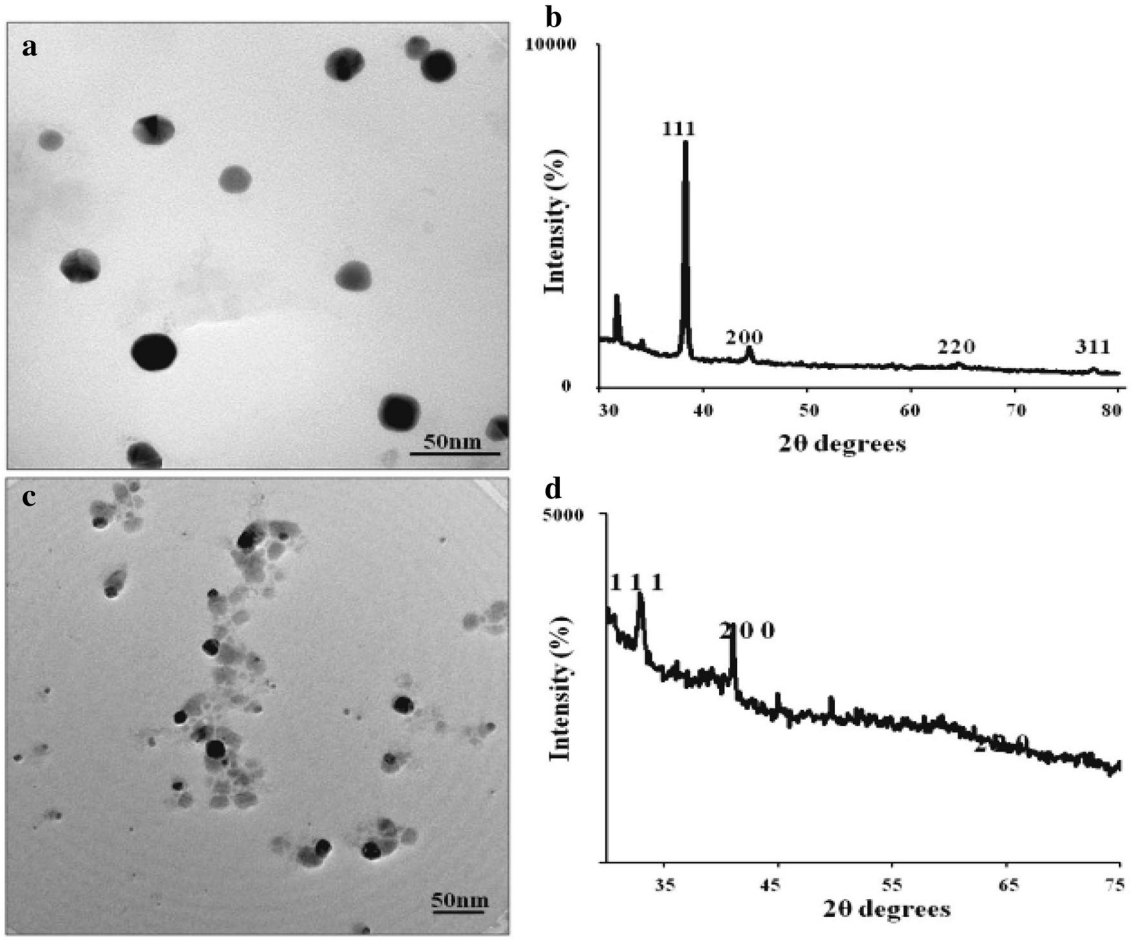

Fig. 6 Characterization of the AuNPs and AgNPs synthesized by purified glycolipid of *W. saturnus* **a** TEM image of AuNPs, **b** XRD profile of AuNPs, **c** TEM image of AgNPs, **d** XRD profile of AgNPs

scavenging potency of the AuNPs was around 40% and was almost similar for all the samples studied. The average percentage inhibition displayed by AgNPs was 50%.

Catalytic applications of extracellular AuNPs and AgNPs

In the present study, extracellular AuNPs and AgNPs were evaluated for their catalytic application for the conversion of 4-NP to 4-AP. On addition of the bio-inspired AuNPs and AgNPs, there was a rapid decrease in the peak intensity at 400 nm (Fig. 7a, b; black arrow) and a concomitant appearance of a peak at 298 nm (Fig. 7a, b; gray arrow). This indicated that the 4-NP was reduced to 4-AP. Control reactions were maintained by replacing NPs with distilled water. In such reactions, the peak at 400 nm was unaltered even after 2 days of incubation. Both the type of nanoparticles were able to bring about catalytic reduction of 4-NP to 4AP.

Discussion

In an attempt to understand the effect of salinity on synthesis of nanoparticles in the current investigation, *W. saturnus* was used as a model system. The yeast tolerated higher concentration of NaCl in a nutritionally rich medium (Fig. 1). The morphology of halotolerant yeasts is often altered in the presence of NaCl (Kralj Kuncic et al. 2010). In the presence of NaCl, the size of *W. saturnus* was found to be smaller (Fig. 2b). This is in agreement with earlier reports on yeasts such as *Yarrowia lipolytica* and *Debaromyces nepalensis* (Andreishcheva et al. 1999; Kumar and Gummadi 2009). In response to salinity stress, certain fungi are known to produce enhanced quantities of pigments such as melanin (Pedras and Yu 2009). *W. saturnus* displayed higher contents of a dark colored pigment in the presence of salt (Fig. S1, supplementary material). On the basis of the major peaks observed in the UV–Visible spectra (Fig. 3) it was concluded that the extracted pigment was melanin (Meredith and Sarna 2006). The high degree

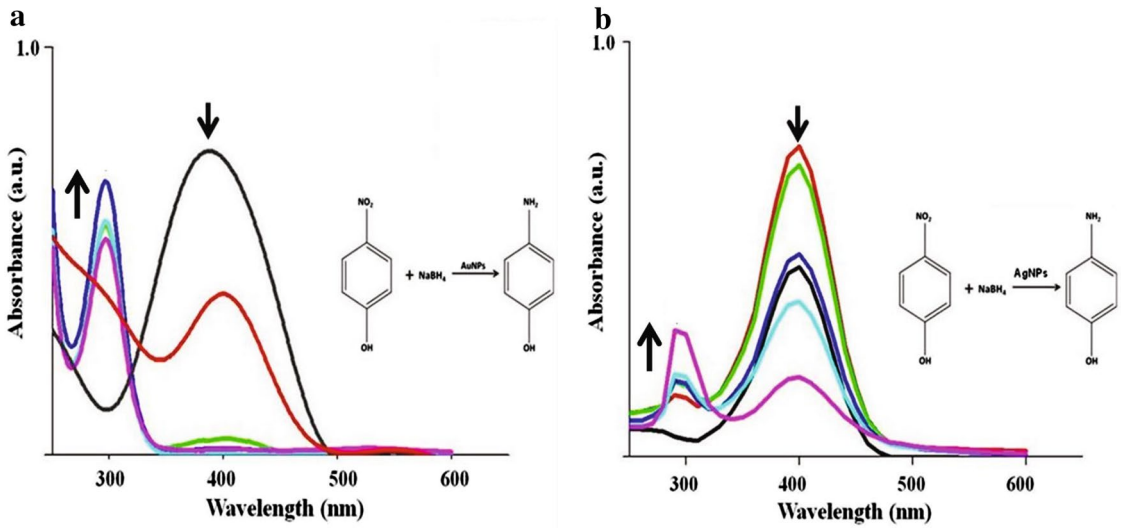

Fig. 7 Catalytic activities of AuNPs and AgNPs. UV–Visible spectra of 4-Nitrophenol reduction reaction mixtures by $NaBH_4$ in the presence of **a** AuNPs, **b** AgNPs over a period of time. *Downward arrows* indicate a decrease in content of 4-NP and the upward arrows depict synthesis of 4-AP over a period of time. *Insets* depict the reactions involved

of resemblance in main FTIR peaks for standard melanin and test samples were observed (Table 1). These spectral details matched with those observed for melanin (Sajjan et al. 2010; Rani et al. 2013; Apte et al. 2013). Physical and chemical tests thus confirmed the effectiveness of the selective protocol in isolating melanin. It is a well-known fact that fungal melanins display strong antioxidant properties. Melanin protects fungal cells from stress conditions induced by high temperature, radiation, salt, free radicals and metals (Fogarty and Tobin 1996; Jacobson 2000). In addition, this pigment has an important role in sequestration of metals and in the synthesis of nanoparticles (Bankar et al. 2009; Apte et al. 2013).

All samples of extracted melanin mediated the synthesis of AuNPs and AgNPs (Fig. S2). Earlier reports have also demonstrated the ability of melanin in forming nanoparticles (Apte et al. 2013; Nair et al. 2013). The yield of melanin increased as the cells were grown in the presence of 0–4% NaCl and this resulted in a decrease in size of nanoparticles (Fig. 5). Higher contents of reducing agents are known to alter the size of NPs (Pimprikar et al. 2009). The melanin stabilized NPs displayed antioxidant properties as detailed later.

Williopsis saturnus also formed AuNPs and AgNPs in an extracellular manner (Fig. S3, supplementary material). AuNPs were found to be hexagonal and spherical (Fig. 5a). Microorganisms are known to mediate the synthesis of nanoparticles that vary in shape and size (Hosseini-Abari et al. 2013; Wadhwani et al. 2014).

In *W. saturnus* NCIM 3298, a glycolipid was found to be responsible for synthesizing extracellular NPs. In literature there are a few reports on glycolipids mediating the synthesis of nanoparticles (Kiran et al. 2010; Apte et al. 2016). To the best of our knowledge, there are no reports on *W. saturnus* species producing glycolipids although some other yeast genera are known to produce them. *Candida* species synthesize sophorolipids and cellobiose lipids are produced by C*ryptococcus* and *Pseudozyma* species (Bhardwaj et al. 2013; Morita et al. 2011, 2013). The glycolipid derived from *W. saturnus* retained its metal reducing activity at high temperatures (boiling water baths) indicating its heat stable nature. Some other microbial glycolipids are also reported to be heat stable (Johnson and Boese-Marrazzo 1980; Sowani et al. 2016a; Mohite et al. 2016). In the presence of NaCl, the glycolipid obtained from *W. saturnus* lost its ability to form NPs (Fig. S5). The glycolipid produced by *Lactobacillus pentosus* is also reported to be salt sensitive (Bello et al. 2012).

The antioxidant and catalytic applications of melanin and glycolipid stabilized NPs, respectively, were also studied (Fig. S6, supplementary material; Fig. 7). Some pigments of microbial origin are known to display antioxidant activities (Gupta et al. 2013; Vora et al. 2014). Moreover, pigment stabilized NPs are also reported for their free radical scavenging activities (Sowani et al. 2016b). Melanin stabilized AuNPs and AgNPs displayed antioxidant properties (Fig S6). Extracellular AuNPs and AgNPs were effective catalysts mediating the reduction of 4-NP to 4-AP (Fig. 7). This reduction reaction occurred under alkaline conditions and involved the intermediate formation of the 4-nitrophenolate ion with an absorption maximum of 400 nm (Zhang et al. 2016). In such reactions, NPs are known to facilitate electron relay from the donor (BH_4^-) to the acceptor (4-NP) by overcoming the kinetic barrier

(Gangula et al. 2011). Biosynthesized AuNPs and AgNPs from other sources are also known to be effective in reducing 4-NP (Wu et al. 2015; Prasad et al. 2015).

Conclusions

In conclusion, cells of the biotechnologically relevant yeast *W. saturnus* were efficient as microbial factories mediating the rapid synthesis of gold and silver nanoparticles in a cell associated and extracellular manner. The nanoparticles were characterized by a variety of analytical techniques and were generally spherical and polycrystalline. Nanoparticles synthesized by using extracted melanin (obtained from cells grown in the absence or presence of NaCl) were monodisperse and displayed DPPH radical scavenging activity. Parameters for extracellular synthesis of nanoparticles were optimized. The nanoparticles synthesized by using CFS under optimum conditions were hexagonal or spherical and polycrystalline in nature. Mechanistic aspect of nanoparticle synthesis was studied by following an activity-guided purification protocol. The moiety present in the CFS mediating the extracellular synthesis of nanoparticles was found to be a salt sensitive glycolipid with glucose as the glycone component, and the aglycone part was made up of palmitic and stearic acid. The AuNPs and AgNPs exhibited good catalytic properties and rapidly mediated the $NaBH_4$-based reduction of 4-nitrophenol to 4-aminophenol. This study suggested that the nanoparticles could potentially be used as antioxidants and catalysts in the cosmetic and pharmaceutical industries.

Funding This work was supported by funds from University Grants Commission under University with Potential for excellence, Phase II. Pallavi Mohite thanks Council of Scientific and Industrial Research (CSIR), New Delhi, India for senior research fellowship.

Compliance with ethical standards

Conflict of interest The authors declare that they have no conflict of interest.

References

Andreishcheva EN, Isakova EP, Sidorov NN, Abramova NB, Ushakova NA, Shaposhnikovl GL, Soares MIM, Zvagilskaya RA (1999) Adaptation to salt stress in a salt-tolerant strain of the yeast *Yarrowia lipolytica*. Biochem (Moscow) 9:1061–1067

Apte M, Girme G, Nair R, Bankar A, Kumar AR, Zinjarde S (2013) Melanin mediated synthesis of gold nanoparticles by *Yarrowia lipolytica*. Mater Lett 95:149–152

Apte M, Chaudhari P, Vaidya A, Kumar AR, Zinjarde S (2016) Application of nanoparticles derived from marine *Staphylococcus lentus* in sensing dichlorvos and mercury ions. Colloids Surf A 501:1–8

Balakumaran MD, Ramachandrana R, Balashanmugama P, Mukeshkumar DJ, Kalaichelvan PT (2016) Mycosynthesis of silver and gold nanoparticles: Optimization, characterization and antimicrobial activity against human pathogens. Microbiol Res 182:8–20

Bankar AV, Kumar AR, Zinjarde SS (2009) Environmental and industrial applications of *Yarrowia lipolytica*. Appl Microbiol Biotechnol 84:847–865

Bello XV, Devesa-Rey R, Cruz JM, Moldes AB (2012) Study of the synergistic effects of salinity, pH, and temperature on the surface-active properties of biosurfactants produced by *Lactobacillus pentosus*. J Agric Food Chem 60:1258–1265

Bhardwaj G, Cameotra SS, Chopra HK (2013) Biosurfactants from Fungi: A Review. J Pet Environ Biotechnol 4:6

Bhattacharya I, Bezawada J, Yan S, Tyagi RD (2015) Optimization and production of silver-protein conjugate as growth inhibitor. J Bionanosci 9:1–9

Fogarty RV, Tobin JM (1996) Fungal melanins and their interactions with metals. Enzym Microb Technol 19:311–317

Gangula A, Podila R, Ramakrishna M, Karnam L, Janardhana C, Rao AM (2011) Catalytic reduction of 4-nitrophenol using biogenic gold and silver nanoparticles derived from *Breynia rhamnoides*. Langmuir 27:1

Gunde-Cimerman N, Zalar P, de Hoog S, Plemenitas A (2000) Hypersaline waters in salterns—natural ecological niches for halophilic black yeasts. FEMS Microbiol Ecol 32:235–240

Gupta C, Prakash D, Gupta S (2013) Functional foods enhanced with microbial antioxidants. Acad J Nutr 2:10–18

Hosseini-Abari A, Emtiazi G Ghasemi SM (2013) Development of an eco-friendly approach for biogenesis of silver nanoparticles using spores of *Bacillus athrophaeus*. World J Microbiol Biotechnol 29:2359–2364

Ito H, Inouhe M, Tohoyama H, Joho M (2007) Characteristics of copper tolerance in *Yarrowia lipolytica*. BioMetals 20:773–780

Jacobson ES (2000) Pathogenic roles for fungal melanins. Clin Microbiol Rev 13:708–717

Jha AK, Prasad K, Prasad K (2009) A green low-cost biosynthesis of Sb_2O_3 nanoparticles. Biochem Eng J 43:303–306

Johnson M, Boese-Marrazzo DI (1980) Production and properties of heat-stable extracellular hemolysin from *Pseudomonas aeruginosa*. Infect Immun 29:1028–1033

Kamat S, Gaikwad S, Kumar AR, Gade WN (2013) Xylitol production by *Cyberlindnera* (*Williopsis*) *saturnus*, a tropical mangrove yeast from xylose and corn cob hydrolysate. J App Microbiol 115:1357–1367

Khodashenas B, Ghorbani HR (2015) Synthesis of silver nanoparticles with different shapes. Arabian J Chem. doi:10.1016/j.arabjc.2014.12.014

Kiran G, Sabu A, Selvin J (2010) Synthesis of silver nanoparticles by glycolipid biosurfactant produced from marine *Brevibacterium casei* MSA19. J Biotechnol 148:221–225

Kowshik M, Deshmukh N, Vogel W, Urban J, Kulkarni SK, Paknikar KM (2002a) Microbial synthesis of semiconductor CdS nanoparticles, their characterization, and their use in the fabrication of an ideal diode. Biotechnol Bioeng 78:583–588

Kowshik M, Vogel W, Urban J, Kulkarni SK, Paknikar KM (2002b) Microbial synthesis of semiconductor PbS nanocrystallites. Adv Mater 14:815–818

Kralj Kuncic M, Kogej T, Drobne D, Gunde-Cimerman N (2010) Morphological response of the halophilic fungal genus *Wallemia* to high salinity. App Env Microbiol 76:329–337

Kumar S, Gummadi SN (2009) Osmotic adaptation in halotolerant yeast, *Debaryomyces nepalensis* NCYC 3413: role of osmolytes and cation transport. Extremophiles 13:793–805

Meredith P, Sarna T (2006) The physical and chemical properties of eumelanin. Pigment Cell Res 19:572–594

Mittal AK, Kaler A, Banerjee UC (2012) Free radical scavenging and antioxidant activity of silver nanoparticles synthesized from flower extract of *Rhododendron dauricum*. Nano Biomed Eng 4:118–124

Moghaddam AB, Namvar F, Moniri M, Tahir PM, Azizi S, Mohamad R (2015) Nanoparticles biosynthesized by fungi and yeast: A review of their preparation, properties, and medical applications. Molecules 20:16540–16565

Mohite P, Apte M, Kumar AR, Zinjarde S (2015) Marine organisms in nanoparticle synthesis. In: Kim SK (ed) Springer handbook of marine biotechnology, Biomedical applications of marine biotechnology. Springer, Berlin Heidelberg, pp 1229–1245

Mohite P, Apte M, Kumar AR, Zinjarde S (2016) Biogenic nanoparticles from *Schwanniomyces occidentalis* NCIM 3459: mechanistic aspects and catalytic applications. App Biochem Biotechnol 179:583–596

Morita T, Ishibashi Y, Fukuoka T, Imura T, Sakai H, Abe M, Kitamoto D (2011) Production of glycolipid biosurfactants, cellobiose lipids, by *Cryptococcus humicola* JCM 1461 and their interfacial properties. Biosci Biotechnol Biochem 75:1597–1599

Morita T, Fukuoka T, Imura T, Kitamoto D (2013) Accumulation of cellobiose lipids under nitrogen limiting conditions by two ustilaginomycetous yeasts, *Pseudozyma aphidis* and *Pseudozyma hubeiensis*. FEMS Yeast Res 13:44–49

Nair V, Sambre D, Joshi S, Bankar A, Kumar AR, Zinjarde S (2013) Yeast-derived melanin mediated synthesis of gold nanoparticles. J Bionanosci 7:159–168

Nghia N, Truong NNK, Thong NM, Hung NP (2012) Synthesis of nanowire-shaped silver by polyol process of sodium chloride. Int J Mater Chem 2:75–78

Oren A (2002) Halophilic microorganisms and their environments. Kluwer Scientific Publishers, Dordrecht

Pedras MS, Yu Y (2009) Salt stress induces production of melanin related metabolites in the phytopathogenic fungus *Leptosphaeria maculans*. Nat Prod Commun 4:53–58

Peng Y, Chi ZM, Wang XH, Li J (2009) Purification and molecular characterization of exo-β-1, 3-glucanases from the marine yeast *Williopsis saturnus* WC91-2. App Microbiol Biotechnol 85:85–94

Pimprikar PS, Joshi SS, Kumar AR, Zinjarde SS, Kulkarni SK (2009) Influence of biomass and gold salt concentration on nanoparticle synthesis by the tropical marine yeast *Yarrowia lipolytica* NCIM 3589. Colloids Surf B 74:309–316

Prasad CH Srinivasulu K, Venkateswarlu P (2015) Catalytic reduction of 4-nitrophenol using biogenic silver nanoparticles derived from papaya (*Carica papaya*) peel extract. Ind Chem 1:104

Rani HSS, Ramesh JT, Subramanian SM (2013) Production and characterization of melanin pigment from halophilic black yeast *Hortaea werneckii*. Int J Pharma Res Rev 2:9–17

Sajjan SS, Kulkarni GB, Yaligara V, Kyoung L, Karegoudar TB (2010) Purification and physiochemical characterization of melanin pigment from *Klebsiella* sp. GSK. J Microbiol Biotechnol 20:1513–1520

Singh P, Kim YJ, Zhang D, Yang DC (2016) Biological synthesis of nanoparticles from plants and microorganisms. Trends Biotechnol 34:588–599

Sowani H, Mohite P, Munot H, Shouche Y, Bapat T, Kumar AR, Kulkarni M, Zinjarde S (2016a) Green synthesis of gold and silver nanoparticles by an actinomycete *Gordonia amicalis* HS-11: mechanistic aspects and biological application. Process Biochem 51:374–383

Sowani H, Mohite P, Damle S, Kulkarni M, Zinjarde S (2016b) Carotenoid stabilized gold and silver nanoparticles derived from the actinomycete *Gordonia amicalis* HS-11 as effective free radical scavengers. Enzym Microb Technol 95:164–173

Sprott GD, Larocque S, Cadotte N, Dicaire CJ, McGee M, Brisson JR (2003) Novel polar lipids of halophilic eubacterium *Planococcus* H8 and archaeon *Haloferax volcanii*. Biochim Biophys Acta 1633:179–188

Tresner HD, Hayes JA (1971) Sodium chloride tolerance of terrestrial fungi. Appl Microbiol 22:210–213

Vadkertiova R, Slavikova E (2006) Metal tolerance of yeasts isolated from water, soil and plant environments. J Basic Microbiol 46:145–152

Vora JU, Jain NK, Modi HA (2014) Extraction, characterization and application studies of red pigment of halophile *Serratia marcescens* KH1R KM035849 isolated from Kharaghoda soil. Int J Pure App Biosci 2:160–168

Wadhwani SA, Shedbalkar UU, Singh R, Karve MS, Chopade BA (2014) Novel polyhedral gold nanoparticles: green synthesis, optimization and characterization by environmental isolate of *Acinetobacter* sp.SW30. World J Microbiol Biotechnol 30:2723–2731

Wu S, Yan S, Qi W, Huang R, Cui J, Su R, He Z (2015) Green synthesis of gold nanoparticles using aspartame and their catalytic activity for *p*-nitrophenol reduction. Nanoscale Res Lett 10:213

Zhang X, Qu Y, Shen W, Wang J, Li H, Zhang Z, Li S, Zhou J (2016) Biogenic synthesis of gold nanoparticles by yeast *Magnusiomyces ingens* LH-F1 for catalytic reduction of nitrophenols. Colloid Surf A 497:280–285